Time resolved nanosecond vortex dynamics in high T_c superconducting films

H. Ferrari [a,1], D. Ibaceta [a], V. Bekeris [a,1], E. Calzetta [a,1], L. Correra [b]

[a] *Departamento de Física, Universidad Nacional de Buenos Aires, Pabellón I, Ciudad Universitaria, Laboratorio de Bajas Temperaturas, (1428) Buenos Aires, Argentina*
[b] *C.N.R.-L.A.M.E.L., Via Gobetti 101, 40129, Bologna, Italy*

Abstract

Flux dynamics in a high T_c superconducting thin film is investigated in the ns time scale. The initial metastable state is determined by applying a pulsed magnetic field to a sample previous cooled below the irreversibility line. Selective local heating of the film with a pulsed laser spot lowers the vortex pinning force suddenly. The magnetic flux rearrangements that follow generate a voltage pulse between two contacts on the zero current biased sample. Detail simulations were performed in the framework of a phenomenological model based on Maxwell Equations with constitutive relations for creep and flux flow that fully describe the observed voltage signals.
© 2003 Elsevier Ltd. All rights reserved.

Keywords: Flux pinning; Flux creep; Vortex dynamics; Critical currents

1. Introduction

Vortex dynamics in type II superconductors continues to be a stimulating research area. Striking memory effects and dynamical ordering of vortex matter in the low frequency domain have been observed recently [1], and may lead in the future to new switching devices [2]. However, the high frequency response of vortex matter is still an open question that needs to be addressed.

In the past, the use of conventional techniques has limited the observation of magnetic properties due to the long intrinsic response and initial data-acquisition times, somewhere between fractions of seconds and minutes [3]. The study of short-time vortex dynamics with novel nonconventional techniques is a requirement to extend the experimental time window towards shorter time scales.

Local techniques that make use of miniature Hall probe arrays [4] and magneto-optical imaging (MOI) have been reported recently to have millisecond time resolution [5–8]. MOI has been further combined with a pulsed laser as the illumination source, reducing the temporal resolution down to the nanosecond time range for the observation of magnetic flux penetration [8]. Interestingly, it has been shown that magnetic field penetrates a superconducting film in form of a homogeneous field gradient or in dendritic magnetic flux avalanches depending on field and temperature [7,8].

In the present work we report on the rearrangement of vortices in high T_c superconducting films over nanosecond time scales observed following the application of a pulsed magnetic field and the subsequent fast heating of the sample at different early stages of the penetration of the field front, in the field and temperature range where the flux penetration is homogeneous [8].

A voltage pulse is induced along the superconducting sample due to the fast flux movement either when the vortices are forced into (out of) the sample by the application (removal) of a magnetic field, or following the partial heating of the sample with a high power pulsed laser beam as it is being penetrated by magnetic field. It should be noted that in these experiments the time resolved voltage signal is recorded, but no current is injected into the sample. The photoinduced voltage is related to the fast motion of vortices [9]. A thermal force cannot explain the results and instead a magnetic force drives flux motion.

_____
E-mail address: hferrari@df.uba.ar (H. Ferrari).
[1] Investigador CONICET.

In earlier work the superconducting film was heated uniformly by a laser pulse at a controlled delay t_d following the application of the pulsed magnetic field, and the flux variation due to sample heating was measured with a pick up coil placed near the film, to determine the short-time magnetization of the sample at t_d, $M(t_d)$ [10–12]. Flux penetration is faster ($\sim$ns) than the pick up coil response time ($\sim$µs), but the time integrated signal is proportional to the difference of the total magnetic flux in the sample at t_d and the total magnetic flux in the sample after it is heated to a temperature above the irreversibility line where $M \sim 0$. The time integral is numerically evaluated and is proportional to $M(t_d)$ (note that the coil's time constant does not determine the time resolution because the relevant information is the time integrated voltage signal induced at t_d in the pick up coil). By repeating the experiment for different delays t_d's, short time magnetic relaxation was investigated [10] and by repeating the experiment at a fixed delay but for different amplitudes of applied magnetic field, the effective critical state magnetization at short times as a function of applied field was studied [11].

To extend the time window towards shorter time scales the starting time t_s, i.e., the shortest delay t_d to trigger the laser pulse after the field pulse is applied, must be reduced. The limitation is determined by the time constant of the measuring array.

In our previous work the starting time was $t_s > 200$ µs. The induced voltage in the pick up coil due to the applied field variation (3 µs rising edge) [12,13] had a characteristic time $\tau = L/R$ determined by the inductive properties of the measuring coil, $L \sim mH$, and the resistive load $R \sim 50$ Ω that matched the internal impedance of the measuring device. The pick up coil was strongly coupled to the applied field (high mutual inductance between primary and secondary coils), so that its variation induced a strong signal (several volts). The pick up coil was not so strongly coupled to the magnetic flux variation that followed the optical heating of the sample and a wide band pre-amplifier was required, that inevitably saturated the measuring device during the initial stages of magnetic field application, and thus masked the photoinduced signal when the laser was triggered at delays shorter than 200 µs.

To reduce the starting time to the microsecond time scale, we have modified the technique of flux movement detection, replacing the pick up coil by a pair of voltage contacts provided on a patterned sample [13]. This detection mode has a lower inductance and as it is optimally coupled to vortex movement the starting time could be reduced to $t_s = 1$ µs, the magnetic field rising edge being the limitation.

In this work we present a full description of the voltage pulse whose time integral no longer scales with the sample magnetization, but provides information related to the flux distribution and mobility. The voltage pulse depends on the constitutive relation $E(J)$ that prevails at each stage. We propose a model to describe vortex dynamics and we simulate numerically the propagation of the field front including vortex creep or flow, and the flux redistribution that follows the fast local reduction of critical current due to heating. We will show that calculations reproduce the measured voltage pulses and describe satisfactorily experimental results after selective heating of the film.

This paper is organized as follows. We first describe the experimental setup and technique, then we present the theoretical model describing the voltage signal that derives from the applied field penetration and the voltages that derive from flux dynamics as a result of partial heating of the sample. We then present our numerical calculations and in the following section results and discussions are presented and conclusions are finally drawn.

2. Experimental

The experimental procedure consists of the preparation of the initial thermomagnetic state by stabilizing the sample temperature below the irreversibility line and applying a transverse pulsed magnetic field H_a at a high rate $dH/dt \sim 1000$ T/s to reduce the uncertainty in the time origin (for a more detailed description see Ref. [10]). Typically the duration of the field pulse, t_h, was 500 µs.

The laser pulse may be triggered at a controlled delay, t_d, which can be varied in each repetition of the experiment to observe the different stages of the propagation of the magnetic field front. Moreover, the laser spot can be optically directed to illuminate different portions of the film and the sample can be heated selectively.

The sample is a $GaBa_2Cu_3O_{7-y}$ film of thickness $\delta = 300$ nm grown by laser ablation on a $NdGaO_3$ substrate. The sample was patterned (see Fig. 2) by laser ablation in the stripe geometry ($\sim 10 \times 2$ mm^2), and voltage contact pads were provided by gold sputtering to reduce contact resistance below 1 Ω. The T_c of the film is 91 K with $\Delta T_c = 1.5$ K (10–90% criterion) determined by ac susceptibility.

For the experimental observations we used a high bandwidth electronic detection method coupled with a pulsed magnetic field generator and a synchronized pulsed laser, based on a previously designed short-time magnetometer [10]. The excimer laser provided 45 ns FWHM pulses at 308 nm and illuminated uniformly an area of 3 cm^2 with 2.5 mJ/cm^2. A slit of controlled width was positioned to illuminate selectively different portions of the sample surface.

Flux penetration can be followed, as will be described below, by measuring the voltage signal across a pair of contacts provided in the film. Fig. 1 shows a schematic
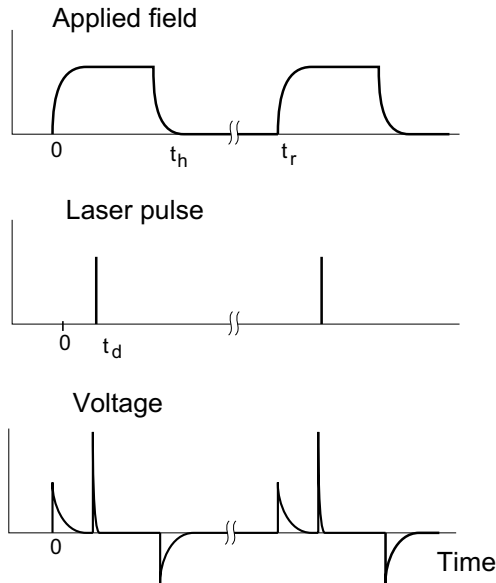
Fig. 1. Schematic time line of events, showing the application of the magnetic field pulse of length t_h at a repetition rate t_r. The laser pulse is synchronized at a delay t_d after the application of the field. The magnetic field rising edge defines the time origin. The voltage signals related to the application/removal of magnetic field and to the optical heating of the sample are shown schematically.

time line that indicates the sequence of events: application of the magnetic field with pulse of length t_h, application of the laser heating pulse at a delay t_d, and detection of the voltage pulse $V(t)$ that results from vortex dynamics; also shown is the repetition time t_r. The repetition rate ($1/t_r \sim 1$ Hz) is limited by the thermal constants of the experimental setup, and is low enough to allow the sample attain its original low temperature before the next magnetic field pulse is applied. The calculated thermal constant resulted in $\sim$10 μs for the sample to attain its original low temperature after the laser pulse is applied [9]. In this work we will refer only to experiments in which $t_d < t_h$. We shall not discuss the heating of the sample in remanent state, i.e., for delays larger than the magnetic field pulse duration, as has been discussed in Ref. [13], although there is no fundamental difference.

The optical heating lowers the pinning force on the vortex structure (at the location where the laser spot is positioned) below that corresponding to the critical state at uniform temperature. This allows the fast penetration of vortices and triggers the flux redistribution in the whole sample. The voltage pulse that results from this flux redistribution at t_d is $\sim$20 ns long, while the voltage signal induced by the application/removal of the magnetic field has a characteristic time of 3 μs, in coincidence with the rising/falling edge of the field pulse. The voltage level of the photoinduced signal ($\sim$500 mV) is about 10 times greater than the signal induced by the changing magnetic field. This signal level, together with

the short-time constant of the measuring circuit, thus provides the possibility of reducing the starting time t_s to below the μs time scale.

3. Theoretical

The superconducting film is modeled as a long strip in a perpendicular magnetic field as schematically shown in Fig. 2. Assuming homogeneity in the z direction and uniform applied transverse magnetic field in the x direction, the voltage reading is given by [14]:

$$\frac{V}{L} = E_b + d\frac{dB_a}{dt} + \int_a^{a+d} \frac{dB_j}{dt}\,dy \qquad (1)$$

where E_b is the electric field at the contacts edge of the strip, B_a is the applied induction field, B_j is the field produced by the current distribution, L and d are the dimensions of the ABCD measuring loop, which connects points A and B on the sample to the voltage measuring device at C and D. We are considering that the lower critical field $H_{c1} = 0$, so that the Meissner state is neglected. The electric field E_b can be interpreted as given by the Josephson relation [15] $E = -v \times B$, where v is an average vortex velocity and B the macroscopic magnetic induction. The first term in Eq. (1) is a superposition of voltage pulses produced by individual vortices moving across the edge, each contributing in one flux quantum, ϕ_0, to the time integral of $V(t)$. The last term in Eq. (1) is the contribution from the change of the flux through the ABCD loop due to the return flux from the vortices. A moving vortex that enters the sample from the left will contribute only to this term.
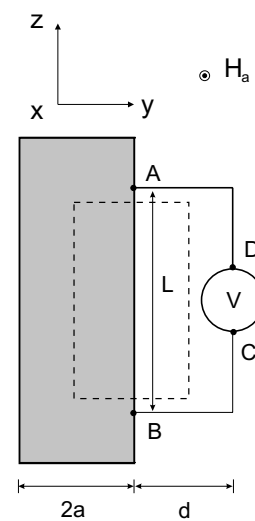

Fig. 2. Experimental setup schematic. The sample is modelized as a strip of width $2a$. The measuring loop ABCD area is $L \times d$. The magnetic field is perpendicular to the sample. No current is injected. The dashed line represents the laser spot.

The magnetic field is given by Ampère's law, resulting in the x component of the magnetic field the following expression,

$$H_x(0,y,0) = H_a + \frac{1}{2\pi}\int_{-a}^{a}\frac{J(y)\mathrm{d}u}{u-y} \qquad (2)$$

Assuming a phenomenological relationship between the electric field and the current density $E = E(J, H, T)$, we will show that the basic features of the experimental results are well described by the quasi-stationary Maxwell equation [16]:

$$\frac{\mathrm{d}E}{\mathrm{d}t} = -\mu_0\left(\frac{\mathrm{d}H_a}{\mathrm{d}t} + \frac{\delta}{2\pi}\int_{-a}^{a}\frac{\mathrm{d}J}{\mathrm{d}t}\frac{\mathrm{d}u}{u-y}\right) \qquad (3)$$

Our experiment samples both the high and low current response of the material. In the high current regime (above the critical state current density J_c), the resistivity takes the flux flow value $\rho_{ff} = \rho_n H/H_{c2}$, where H is the local field, H_{c2} is the upper critical field, and ρ_n is the normal state resistivity. In the low current regime, $J < J_c$, the resistivity is due to thermally activated creep and results in an electric field of the form [16] $E = E_c(J/J_c)^n$, where $n \gg 1$. Note that the resistivity at each point depends on the local magnetic field, which in turn is sensitive to the current distribution over the whole sample, leading to highly nonlinear and nonlocal dynamics. The temperature dependence of the critical current is given by [17] $J_c(T) = J_{c0}(1 - T/T_i)^{3/2}$. For $H_a = 7500$ A/m, the observed irreversibility temperature (above which no photosignal is detected) is $T_i = 86$ K. For the critical field in the region under study we can approximate [18] $H_{c2} = (T_c - T)1.8 \times 10^6$ A m^{-1} K^{-1}.

For the temperature independent parameters of these simulations we choose $n = 20$, $\delta J_{c0} = 25$ kA/m, $\rho_n/\delta = 100$ Ω and $E_c = 0.01$ V/m. All measurements (and calculations) were made at an initial temperature $T_0 = 73.2$ K. The time-dependent temperature that results after local optical heating (see below) determines the time dependence of J_c and H_{c2}.

To account for the experimental data we must assume that the cross-over from one current regime to the other is smooth. We achieve this by interpolating both regimes with a cubic form in a small range $\sim 5\%$ J_c.

Phenomenological constitutive relations of the kind we have discussed break down in the limit of very weak magnetic fields, i.e., when we are dealing with regions of the sample where the magnetic flux has not yet penetrated. For this reason, we assume that there is a cut-off in the constitutive relation such that $E = 0$ whenever $H < H_1$, with $H_1 = 10^{-8}\,H_{c2}$. This regime is relevant to the early stages of the simulation.

The resulting nonlinear nonlocal magnetic flux diffusion equation was integrated numerically by means of a time adaptive algorithm for the generally nonsymmetric sheet current distribution [19] $\delta J(y,t)$. In the

following section we present our theoretical and experimental results.

4. Results and discussion

We first calculated the spatial distribution inside the sample of the sheet current density, the magnetic field profile and the vortex velocity at different times after triggering the laser pulse, following the application of the magnetic field. In calculations we have used the experimental value for the applied magnetic field: $H_a = 7500$ A/m with a rising edge modeled as an algebraic initial slope followed by an exponential time dependence with a characteristic rise time $\tau \sim 3.5$ μs.

Illumination of the two thirds of the sample surface on the side of the contacts (right side of the sample in Fig. 2) 4 μs after the application of the field produces a local temperature rise. The local temperature rise reduces the local critical current density below the flowing current density value (we neglect lateral thermal diffusion that would represent an increase in temperature in an additional small percentage of the illuminated area during the duration of the pulse). This leads to a rapid reduction of sheet current density and the corresponding penetration of magnetic flux.

Observe that a possible temperature dependence in the creep exponent, n, would not affect our measurements since in the cold zone temperature is essentially constant, and in the hot zone the sheet current is above the critical sheet current density leading to vortex flux flow regime.

The temperature time dependence at the laser spot for these simulations is:

$$\frac{T - T_0}{T_i} = A\frac{(t/C)^N}{1 + \frac{N}{M-N}(t/C)^N} \qquad (4)$$

where T_0 and T_i are the initial and the irreversibility temperatures, and t is the time elapsed since the laser pulse is triggered. The parameter values are $N = 4$, $C = 15$ ns, $M = 4.3$ and $A = 2.8$.

The essential feature of this dependence is the asymmetry between the fast heating and the slow cooling of the illuminated area. This behavior has been observed in simulations of heat diffusion for realistic values of diffusion coefficients of sample and substrate and sample thickness [9]. The particular values of the coefficients in Eq. (4) follow from a global fit to the experimental data. Observe that temperature rises from the initial value $T_0 = 73.2$ K to $T_{max} = 90$ K, which is higher than the irreversibility temperature $T_i = 86$ K.

From the numerical solution of the evolution equation (Eq. (3)), with the constitutive relation already discussed, we have reconstructed the time evolution of the sheet current and the magnetic and electric fields
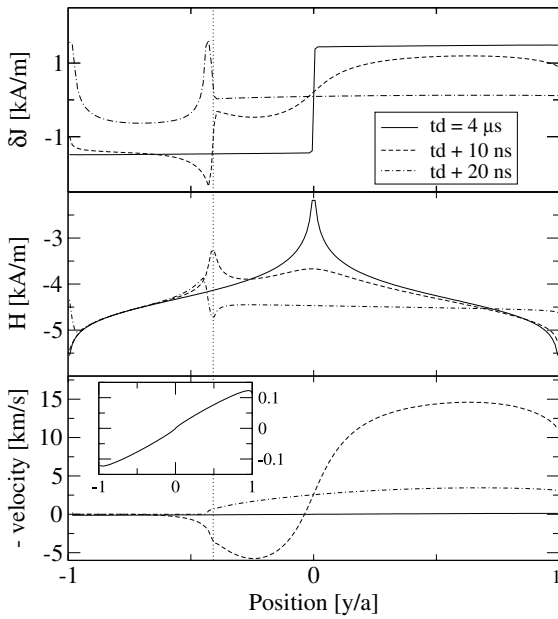
Fig. 3. Space distribution of sheet current density (upper), magnetic field and vortices velocities (lower); for different times since the start of the laser pulse.

inside the sample. Also, assuming the Josephson relation $E = -v \times B$, we have obtained the mean velocity field of the vortices within the sample.

In Fig. 3 we show the calculated sheet current distribution (upper panel) at different times since the triggering of the laser pulse.

The time origin was arbitrarily chosen at the instant where the voltage signal induced by the application of the magnetic field reaches its maximum (see also Fig. 4).
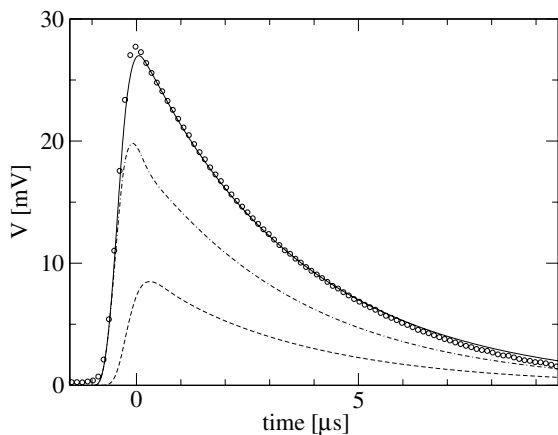

Fig. 4. Observed and simulated signal for the turning-on of the applied field. The time origin was arbitrarily chosen at the instant where the voltage signal induced by the application of the magnetic field reaches its maximum. From bottom to top, the lines represent the contribution of the electric field at the edge of the film, the contribution due to the flux variation into the ABCD loop, and the total signal. The circles are the observed values.

The vertical dotted line indicates the border between cold (left) and heated (right) areas. We also show the magnetic field (middle panel) and the velocity field (lower panel) at the corresponding times. Observe that a positive sign in this last plot represents left moving vortices, while the applied field points in the negative x direction. Note that the velocities after heating reach values of the order 10^4 m/s and before heating 10^2 m/s. To appreciate the different scales we have inserted in the lower panel the plot of the initial velocities with a higher resolution. At t_d the velocities are odd functions of position because the applied field is homogeneous. The calculated mean velocities are consistent with earlier observations of propagation of flux fronts [8]. In conventional flux creep experiments where the time scale is ~ 10 s vortex velocity is estimated to be $v \sim 0.1$ m/s.

We will refer now to the calculated and the measured voltage signals induced by the application of the magnetic field and by the partial heating of the sample.

Fig. 4 shows the voltage signal induced by the application of 7500 A/m. The experimental magnetic field rising edge was approximately exponential with a characteristic rise time $\tau \sim 3.5$ μs. Symbols indicate the measured voltage, and in full line we show the calculated voltage signal induced by an algebraic initial slope followed by an exponential rising edge for the simulated applied field. The lower signals, from bottom to top, correspond to the calculated voltage associated to the electric field at the edge of the sample, and the contribution due to flux variation in the ABCD measuring loop, following Eq. (1).

Observe the delay in the onset of the edge electric field, associated with the formation of the characteristic current profile. Once formed, the model predicts the contacts voltage to be proportional to dH_a/dt and independent of the sample parameters for the regime where the applied field changes faster than the induced one.

Illumination of the two thirds of the sample surface on the side of the contacts (right side in Fig. 2) 4 μs after the application of the field produced the experimental voltage pulse plotted in Fig. 5 (open circles). Note the different voltage and time scales in Figs. 4 and 5. The local temperature rise reduces the local critical current density below the flowing current density value (we neglect lateral thermal diffusion that would represent an increase in temperature in an additional small percentage of the illuminated area during the duration of the pulse). This leads to a rapid reduction of sheet current density and the correlated penetration of magnetic flux.

The curves plotted in the upper inset of the figure are the calculated voltage signals for this situation. The dashed curve corresponds to the electric field contribution at the sample edge, the negative dotted curve is the term related to the magnetic flux variation through the ABCD measuring loop, and the full line is the total
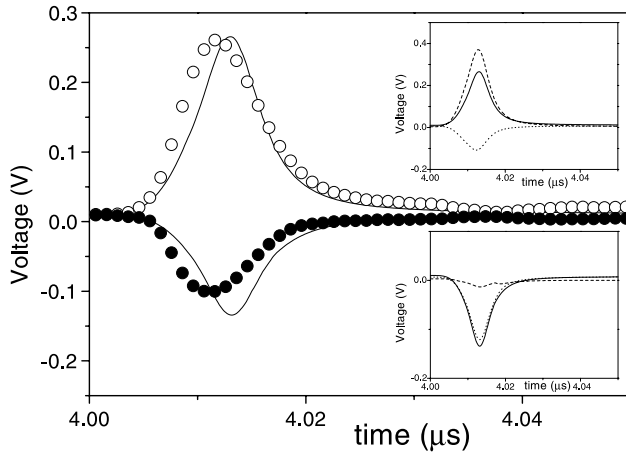
Fig. 5. Voltage signals following the optical heating of the sample on the side of the voltage contacts (open circles) and on the opposite side (full circles). The upper (lower) inset shows the simulated composition of the signals corresponding to right (left) heating. The total voltage in full line (insets and main panel) results from the contribution of the electric field (dashed line) and the flux variation through the ABCD loop (dotted–dashed line). If the left side is heated (far from voltage contacts) almost no vortices enter through the cold side.
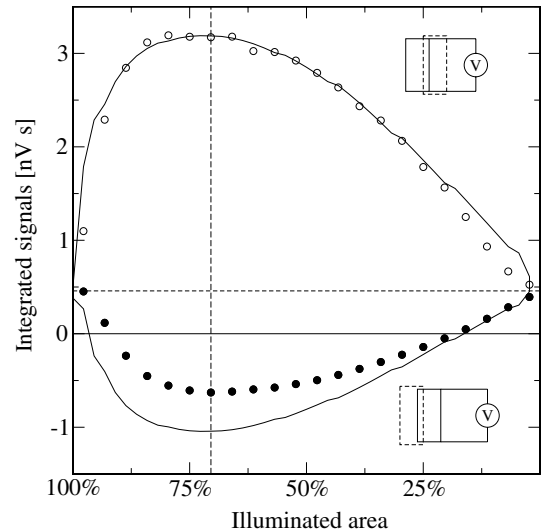

Fig. 6. Scanning of the film, varying the heated area. The circles show the time integrated observed voltage signal as a function of the percentage of the heated area. Empty (full) circles are for heating near (far) the contacts. Full lines are calculations.

calculated voltage signal also shown in full line in the main panel.

In the main panel of Fig. 5, the full circles show the corresponding result when a similar area of the sample is illuminated at the edge opposite to the contacts (the left one). Notice that the measured voltage changes sign. This result is also well described by the calculations which are plotted in the lower inset, where the flux time derivative (dotted negative curve) is almost the only contribution to the total voltage. Indeed, almost no vortices move across the contacts edge as they are magnetically forced to enter into the film from the opposite direction. In this case, therefore, the electric field (dashed line) is a negligible contribution to the total voltage signal plotted in full line in the lower inset and in the main panel.

To test the model further, the laser spot was scanned across the film, repeating the experiment at a fixed temperature and at a fixed delay time t_d. The measured voltage signals were time integrated V_{int} and are plotted in Fig. 6 (circles) as a function of the percentage of heated area of the strip. While the upper half (open circles) corresponds to heating the contacts side of the sample, the lower curve (full circles) corresponds to the heating of the opposite side of the strip. The horizontal dashed line shows the contribution to the voltage signal induced by the application of the magnetic field 4 μs earlier. Note that this contribution is constant for the time scale of the pulse duration. Part of these data were reported earlier in Ref. [13]; but to the best of our knowledge the theoretical interpretation is new.

The fast decay in the critical current produced by heating triggers the rearrangement of the vortices. In

fact, the critical sheet current drops to zero, since the temperature goes over the irreversibility line. While magnetic field penetration occurs mainly from the heated edge of the strip, some vortices enter the illuminated area from the cold edge, meaning that there must be vortex motion in the cold area as well.

5. Conclusions

We have investigated vortex motion in the micro and the nano second time scales. We have shown that a more abrupt change in magnetic field on the sample is accomplished by heating selectively the sample with a laser pulse. By scanning the laser pulse across the sample, delaying the application of the pulse with respect to the application of the external magnetic field, and by heating the sample both on and across the contacts' side, we have been able to observe different aspects of vortex dynamics on nanosecond time scales, and to discriminate between the different contributions to the measured signal. By means of numerical simulations, we have been able to reconstruct the evolution of the current and vortex motion within the sample in these fast time scales satisfactorily, making use of a phenomenological model based on Maxwell Equations and the known constitutive relations for flux creep and flux flow, thus extending the time window for the study of vortex dynamics in HTSC.

References

[1] Gordeev SN et al. Nature 1997;385:324;
Henederson W, Andrei EY, Higgins M. Phys Rev Lett 1998;
81:2352;
Xiao ZL, Andrei EY, Higgins MJ. Phys Rev Lett 1999;83:1664;
Valenzuela SO, Bekeris V. Phys Rev Lett 2000;84:4200;
Valenzuela SO, Bekeris V. Phys Rev Lett 2001;86:504.

[2] Banerjee SS, Patil NG, Ramakrishnan S, Grover AK, Bhattach-
arya S, Ravikumar G, et al. Appl Phys Lett 1999;74:126.

[3] Yeshurun Y, Malozemoff AP, Shaulov A. Rev Mod Phys 1996;
68:911.

[4] Abulafia Y, Shaulov A, Wolfus Y, Prozorov R, Burlachkov L,
Yeshurum Y, et al. Phys Rev Lett 1995;75:2404.

[5] Theuss H, Forkl A, Kronmuller H. Physica C 1992;190:345.

[6] Dorosinskii LA, Indenbom MV, Nikitenko VI, Ossipyan YA,
Polyanskii AA, Vlasko-Vlasov VK. Physica C 1992;203:149.

[7] Johansen TH, Baziljevich M, Shantsev DV, Goa PE, Galperin
YM, Kang WN, et al. Supercond Sci Technol 2001;14:726;
Barkov FL, Shantsev DV, Johansen TH, Goa PE, Kang WN,
Kim HJ, et al. Available: cond-mat/0205361.

[8] Leiderer P, Boneberg J, Brüll P, Bujokand P, Herminghaus S.
Phys Rev Lett 1991;71:2646;
Runge BU, Bolz U, Eisenmenger J, Leiderer P. Physica C
2000;341–348:2029.

[9] Puig T, Huggard PG, Schneider G, O'Brien TP, Blau W, Pont M,
et al. Phys Rev B 1992;46:11240;
Gupta D, Donaldson WR, Kadin AM. J Appl Phys 1995;78:372.

[10] Valenzuela SO, Ferrari H, Bekeris V, Marconi MC, Guimpel J, de
la Cruz F. Rev Sci Instrum 1998;69:251.

[11] Valenzuela SO, Ferrari H, Bekeris V, Guimpel J, de la Cruz F.
Rev Mex Fís 1998;44:193.

[12] Ferrari H. PhD Thesis 2000; Universidad de Buenos Aires.

[13] Ferrari H, Valenzuela SO, Bekeris V, Dediu VA, Correra L.
Supercond Sci Technol 1999;12:210.

[14] Clem JR. Phys Rep 1981;75:1.

[15] Josephson BD. Phys Lett 1962;1:251.

[16] Brandt EH, Indemnbom M. Phys Rev B 1994;48:12893;
Brandt EH. Phys Rev B 1994;49:9024.

[17] Wurlitzer M, Lorenz M, Zimmer K, Esquinazi P. Phys Rev B
1997;55:11816, and references therein.

[18] This is a typical value extracted from Poole CP, Farach HA,
Creswick RJ. Superconductivity. New York: Academic Press;
1995.

[19] Press WH, Teukolsky SA, Vetterling WT, Flannery B. Numerical
Recipes. 2nd ed. Cambridge, UK: Cambridge University press;
1992.